International Journal of Difference Equations (IJDE).
ISSN 0973-6069 Volume 17, Number 2 (2022), pp. 361-377
©Research India Publications
https://www.ripublication.com/ijde.htm

Magnetic Effects on Pulsatile Flow of Copper Suspended Nanofluid Venture Through a Branched Artery

G. Madhava Rao[*1] **and D. Srinivasacharya**[2]

[1]*Department of Mathematics, Malla Reddy University, Hyderabad-500 100, Telangana State, India.*

[2]*Department of Mathematics, National Institute of Technology, Warangal-506004, Telangana State, India*

Abstract

In this article, we demonstarted and characterised the unsteady pulsatile blood flow through a bifurcated artery using blood as copper suspended nanofluid in the presence of applied magnetic field. The governing equations of a nanofluid model are reduced by dealing with the mild stenosis case. A radial coordinate transformation was initiated to transform irregular grid into a well defined grid. Forward time and central space difference scheme was used to calculate the solution for flow rate, resistive impedance and shear stress. As a result of this study we can control the volume of blood using magnetic effect. A quantitative analysis is performed in order to estimate the effects of pertinent parameters on physical quantities by means of graphical representations.

Keywords: Pulsatile blood flow; Copper nanoparticles; Magnetic field; Bifurcated artery; Heat source parameter.

1. INTRODUCTION

The literature of biomechanics and the human cardiovascular system have received many number of applications in the branch of pharmaceutical sciences. Investigation of blood flow characteristics in an artery with mild stenosis and division is very important topic as the number of cardiovascular diseases like heart stroke or attack, brain dead, paralysis are the major cause of deaths. Blood flow characteristics in the complex network system of arteries mainly depends on the shape of artery,

[*]Corresponding author's email ID: rao.gmr.madhav@gmail.com

viscosity and non-Newtonian character of blood and also the performance of flow like laminar or turbulent, pulsatile, microrotation etc.. Accumulation of fatty texture inside the lumen (known as stenosis), which reduces blood flow to some degree. The appreciable amount of attention has been given to the nanofluids research in recent decades due to their important contributions in engineering and biomedical research. Nanoparticles are small in size and having enormous surface areas. Therefore, these fluids have extreme properties like minimal blocking in flow passages, high thermal conductivity, long-term stability, and homogeneity. Due to these reasons, fluids have many number of potential applications in peristaltic pumps for diabetic treatments, pharmacological administration mechanisms, electronics cooling, solar collectors and nuclear applications. Initially, [1] presented the perception of nanofluids for suspension of liquids having extremist particles. Nanofluids inflate heat transfer rate compared to the base fluid has been analysed by [2]. [3] observed that the height of stenosis plays a key role in the variation of impedance in a catheterized tapered artery by overbearing blood as Jeffrey fluid with suspension of nanoparticles. [4] considered the nanofluid flow of blood in obstacle arteries with permeable walls. Impedance to the flow is higher for converged tapering when compared with non-tapered and diverging tapered arteries is mentioned by [5]. [6] discussed ferromagnetic field influence on blood flow through composite stenosed arteries. Effect of magnetic field on copper suspended nanofluid venture through a bifurcated artery without pulsatile nature has been studied by [7]

The philosophy of MHD plays essential role in flow of blood in human arterial system. The numbers of magnetic devices have been invented for drug transporter, treatment of cancer tumor etc. The theory of emf in medical science has been introduced by [8] and then followed by [9]. Heat transmission in blood flow has large number of applications in skin and muscle tissues, thermic therapy and other treatments. [10] considered heat transmission of blood as 3^{rd} grade nanofluid by adding gold nanoparticles to blood in porous media in the presence of a magnetic field. [11] declared that blood flow characteristics are more at the aneurysm segment comparatively with the stenotic region. [12] analysed the influence of nanoparticles on flow of blood inside stenosed artery. Apart from the considerable development for diagnosis and treatment of these diseases, still this field of investigation requires further development.

The present article deals with copper suspended nanofluids for pulsatile flow of blood through a bifurcated artery in the presence of MHD. Variation of temperature, flow rate, impedance and shearing stress are analyzed for different values of pertinent parameters involved in physical problem.

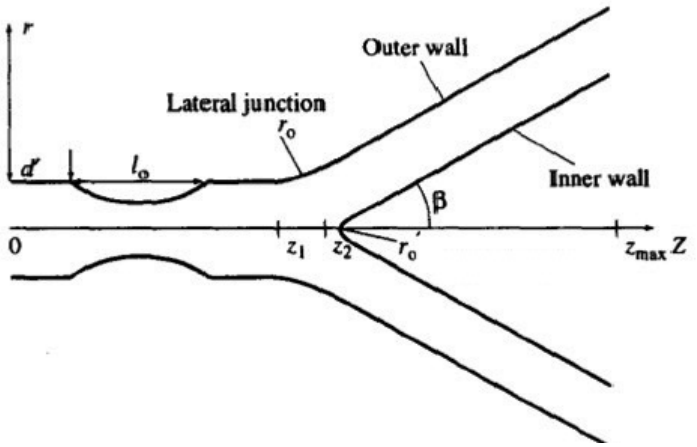

Figure 1: Schematic diagram of stenosed bifurcated artery.

2. MATHEMATICAL FORMULATION

Consider incompressible homogeneous pulsatile flow of blood through a bifurcated artery for which there is a mild stenosis in the parent artery. Design of arteries are assumed to be symmetric about the main axis and parent artery has single mild stenosis as shown in fig. 1. Curvature is imported at the begining of lateral junction and the flow divider therefore opportunity of flow partition areas (if any) can be eliminated. Blood is treated to be pulsatile and copper suspended nanofluid of constant density. The fluid properties are assumed to be constant, except the density, so that the Boussinesq approximation can be used. Let $(r,\ \theta,\ z)$ be any material point in cylindrical polar coordinate system, where $z-$axis is taken along the main axis of the parent artery.

Governing equations for the nanofluid flow through bifurcated artery are

$$\rho_{nf}\left[\frac{\partial \rho}{\partial t}+\frac{\partial u}{\partial r}+\frac{u}{r}+\frac{\partial w}{\partial z}\right]=0 \tag{1}$$

$$\rho_{nf}\left[\frac{\partial u}{\partial t}+u\frac{\partial u}{\partial r}+w\frac{\partial u}{\partial z}\right]=-\frac{\partial p}{\partial r}+\mu_{nf}\frac{\partial}{\partial r}\left[2\frac{\partial u}{\partial r}\right]+\mu_{nf}\frac{\partial}{\partial z}\left[2\frac{\partial u}{\partial z}+\frac{\partial w}{\partial r}\right] \tag{2}$$

$$\begin{aligned}\rho_{nf}\left[\frac{\partial w}{\partial t}+u\frac{\partial w}{\partial r}+w\frac{\partial w}{\partial z}\right]=&-\frac{\partial p}{\partial z}+\mu_{nf}\frac{\partial}{\partial z}\left[2\frac{\partial w}{\partial z}\right]+\\&\frac{\mu_{nf}}{r}\frac{\partial}{\partial r}\left[r(\frac{\partial u}{\partial z}+\frac{\partial w}{\partial r})\right]+\rho_{nf}g\beta_2(T-T_0)-\sigma B_0^2 w\end{aligned} \tag{3}$$

$$(\rho_{cp})_{nf}\left[\frac{\partial T}{\partial t}+u\frac{\partial T}{\partial r}+w\frac{\partial T}{\partial z}\right]=K_{nf}\left[\frac{\partial^2 T}{\partial r^2}+\frac{1}{r}\frac{\partial T}{\partial r}+\frac{\partial^2 T}{\partial z^2}\right]+Q_1 \tag{4}$$

where u,w are the components of velocity along radial and axial axes directions respectively, β_2 is volumetric expansion parameter, g is the gravitational acceleration, Q_1 is heat generation, T is temperature of the fluid, ρ_{nf} is effective density, μ_{nf} is effective dynamic viscosity, B_0^2 is applied magnetic force, $(\rho_{cp})_{nf}$ is heat capacitance and K_{nf} is effective thermal conductivity, these are defined as follows

$$\left.\begin{array}{l} \rho_{nf} = (1-\phi)\rho_f + \phi\rho_f,\ \mu_{nf} = \frac{\mu_f}{(1-\phi)^{2.5}}, \\ (\rho_{cp})_{nf} = (1-\phi)(\rho c_p)_f + \phi(\rho c_p)_s, \\ \alpha_{nf} = \frac{K_{nf}}{(\rho c_p)_{nf}} \\ K_{nf} = K_f \left[\frac{K_s+2K_f-2\phi(K_f-K_s)}{K_s+2K_f+\phi(K_f-K_s)}\right] \end{array}\right\} \tag{5}$$

where α_{nf} is effective thermal diffusivity. In the above expression for effective thermal conductivity does not consider the thermal interface resistance between nanoparticles and fluid. Size of particle and interfacial thermal resistance is combined in calculating effective thermal conductivity. Copper nanoparticle thermal conductivity ($K_s = 401\ Wm^{-1}(K^{-1})$)is more than the base fluid thermal conductivity $K_f = 0.613\ Wm^{-1}(K^{-1})$), therefore ratio K_f/K_s can be approximated as zero [13]. This implise $\frac{K_s+2K_f-2\phi(K_f-K_s)}{K_s+2K_f+\phi(K_f-K_s)} = 1+3\phi$.

The mathematical representation of bifurcated artery under consideration is given by [14, 15]

$$R_1(z,t) = \begin{cases} a\ a_1(t) & 0 \le z \le d^{'} \\ (a - \frac{4\epsilon}{l_0^2}(l_0(z-d^{'}) - (z-d^{'})^2)\ a_1(t) & d^{'} \le z \le d^{'}+l_0 \\ a\ a_1(t) & d^{'}+l_0 \le z \le z_1 \\ (a + r_0 - \sqrt{r_0^2 - (z-z_1)^2})\ a_1(t) & z_1 \le z \le z_2 \\ (2r_1 sec\beta + (z-z_2)tan\beta)\ a_1(t) & z_2 \le z \le z_{max} \end{cases} \tag{6}$$

$$R_2(z,t) = \begin{cases} 0 & 0 \le z \le z_3 \\ (\sqrt{(r_0^{'})^2 - (z-z_3-r_0^{'})^2})\ b_1(t) & z_3 \le z \le z_3 + r_0^{'}(1-sin\beta) \\ (r_0^{'}cos\beta + z_4)\ b_1(t) & z_3 + r_0^{'}(1-sin\beta) \le z \le z_{max} \end{cases} \tag{7}$$

where $R_2(z)$, $R_1(z)$ are inner and outer walls of considered artery, r_1 and a are radius of the daughter and parent arteries, l_0 is length of the stenosis, β is half of the bifurcation angle, ϵ is the ultimate height of the stenosis at $z = d^{'} + l_0/2$ and z_{max} speak for finite length of the artery under consideration, z_1 and z_2 are location of onset and offset of the lateral junction, z_3 is the apex. z_1, z_2 and z_3 are functions of half of the bifurcated angle. These are defined as $z_2 = z_1 + r_0 \sin\beta$, $z_3 = z_2 + q_1$, $z_4 = (z - z_3 - r_0^{'}(1-sin\beta))tan\beta$, q_1 is a small number which is for the rapport of the geometry lies in between 0.1 and 0.5.

and $a_1(t), b_1(t)$ are given by

$$a_1(t) = 1 - (\cos(\omega t) - 1)k\ \exp(-k\omega t),\ b_1(t) = \frac{1}{a_1(t)}$$

The boundary conditions associated with physical problem are:

$$\left.\begin{array}{l} \frac{\partial w}{\partial r} = 0,\ \ \frac{\partial T}{\partial r} = 0,\ \text{ on } r = 0 \text{ for } 0 \le z \le z_3 \\ w = 0,\ \ T = 0,\ \text{ on } r = R_1(z) \text{ for all } z \\ w = 0,\ \ \frac{\partial T}{\partial r} = 0,\ \text{ on } r = R_2(z) \text{ for } z_3 \le z \le z_{max} \\ w = w_0,\ \text{ at initial time.} \end{array}\right\} \tag{8}$$

Since flow is pretend to be commensurate about the axis, all variables are independent of θ. This implies, velocity along radial direction is neglected. Therefore, along flow direction, the variation of all the flow attributes is taken to be zero except pressure [16].

Define the non-dimensional variables as

$$\left.\begin{array}{l} r = a\widetilde{r},\ u = \frac{aw_0\widetilde{u}}{L},\ z = L\widetilde{z},\ w = w_0\widetilde{w},\ d = L\widetilde{d},\ P = \frac{Lw_0\mu_f\widetilde{P}}{a^2}, \Theta = \frac{T}{T_w - T_0}, \\ R_1(z) = a\widetilde{R}_1(\widetilde{z}),\ R_2(z) = a\widetilde{R}_2(\widetilde{z}),\ r_1 = a\widetilde{r}_1,\ z_1 = a\widetilde{z}_1,\ t = \frac{\widetilde{t}}{\omega}, \end{array}\right\} \tag{9}$$

where L is characteristic length and w_0 is characteristic velocity.

Use the non-dimensional variables (9) in equations (1) - (8) and neglecting the tildes, reduces to,

$$\frac{\partial p}{\partial r} = 0 \tag{10}$$

$$\left.\begin{array}{l} R_w^2\ \frac{\partial w}{\partial t}\ =\ -\frac{\partial p}{\partial z} + \frac{1}{(1-\phi)^{2.5}}\left[\frac{\partial^2 w}{\partial r^2} + \frac{1}{r}\frac{\partial w}{\partial r}\right] + \\ G_r\Theta - H^2 w \end{array}\right\} \tag{11}$$

$$R_w^2\ P_r^2\ \frac{\partial \Theta}{\partial t}\ =\ \frac{\partial^2 \Theta}{\partial r^2} + \frac{1}{r}\frac{\partial \Theta}{\partial r} + s\,(1 + 3\phi) \tag{12}$$

$$R_1(z,t) = \begin{cases} a_1 & 0 \le z \le d^{'} \\ (1 - \frac{4\epsilon}{al_0^2}(l_0(z - d^{'}) - (z - d^{'})^2)a_1 & d^{'} \le z \le d^{'} + l_0 \\ a_1 & d^{'} + l_0 \le z \le z_1 \\ (1 + r_0 - \sqrt{r_0^2 - (z - z_1)^2})a_1 & z_1 \le z \le z_2 \\ (2r_1 sec\beta + (z - z_2)tan\beta)a_1 & z_2 \le z \le z_{max} \end{cases}$$

$$R_2(z,t) = \begin{cases} 0 & 0 \le z \le z_3 \\ (\sqrt{(r_0^{'})^2 - (z - z_3 - r_0^{'})^2})b_1 & z_3 \le z \le z_3 + r_0^{'}(1 - sin\beta) \\ (r_0^{'}cos\beta + z_4)b_1 & z_3 + r_0^{'}(1 - sin\beta) \le z \le z_{max} \end{cases}$$

$$\left.\begin{array}{l} \frac{\partial w}{\partial r}=0,\ \ \frac{\partial \Theta}{\partial r}=0,\ \ \text{on}\ \ r=0\ \ \text{for}\ \ 0\leq z\leq z_3 \\ w=0,\ \ \Theta=0,\ \ \text{on}\ \ r=R_1(z)\ \ \text{for all}\ \ z \\ w=0,\ \ \frac{\partial \Theta}{\partial r}=0,\ \ \text{on}\ \ r=R_2(z)\ \ \text{for}\ \ z_3\leq z\leq z_{max}, \\ w=w_0,\ \ \text{at initial time.} \end{array}\right\} \tag{13}$$

where $R_w^2 = \frac{\rho_{nf}\omega a^2}{\mu_f}$ is the Womesley number, P_r represents the Prandtl number, $G_r = \frac{g\beta_2 a^2(T_w-T_0)\rho_{nf}}{w_o\mu_f}$ is the Grashof number and $s = \frac{Q_1 a^2}{k_f(T_w-T_0)}$ is the Heat source parameter.

The pulsatile pressure gradient present in equation (11) is

$$-\frac{\partial p}{\partial z} = A_0 + A_1\cos(\omega t)$$

where A_0 is the constant pressure gradient, A_1 is the amplitude of systolic and diastolic pressure component and $\omega = 2\pi f_p$, f_p is the frequency of pulsatile flow.

The influence of walls of the artery (i.e. $R_1(z,t)$ and $R_2(z,t)$) can be imposed into the governing equations and boundary conditions by using the radial coordinate transformation [17] $\xi = \frac{r-R_2}{R}$, where R(z,t) = $R_1(z,t) - R_2(z,t)$. Using this transformation into equations (11) and (12), take the form

$$R^2\ R_w^2\ \frac{\partial w}{\partial t} = \left[R\ R_w^2\ p(k) + \frac{R}{(1-\phi)^2.5\ (\xi R+R_2)}\right]\ \frac{\partial w}{\partial \xi} - \tag{14}$$

$$R^2\frac{dp}{dz} + \left(\frac{1}{(1-\phi)^{2.5}}\right)\frac{\partial^2 w}{\partial \xi^2} - R^2H^2w + R^2G_r\Theta$$

$$R^2\ R_w^2\ P_r^2\frac{\partial \Theta}{\partial t} = \frac{\partial^2\Theta}{\partial \xi^2} + R^2\ s\ (1+3\phi) + \left[R\ R_w^2\ p(k)\ P_r^2 + \frac{R}{(1-\phi)^{2.5}\ (\xi R+R_2)}\right]\ \frac{\partial \Theta}{\partial \xi} \tag{15}$$

where $p(k) = \frac{\partial R}{\partial t} + \xi\frac{\partial R_2}{\partial t}$ is corresponding to wall motion.

The corresponding boundary conditions in the transformed co-ordinate system are

$$\left.\begin{array}{l} \frac{\partial w}{\partial \xi}=0,\ \ \frac{\partial \Theta}{\partial \xi}=0,\ \ \text{on}\ \ \xi=0\ \ \text{for}\ \ 0\leq z\leq z_3 \\ w=0,\ \ \Theta=0\ \ \text{on}\ \ \xi=1\ \ \text{for all}\ z \\ w=0,\ \ \frac{\partial \Theta}{\partial \xi}=0\ \ \text{on}\ \ \xi=0\ \ \text{for}\ z_3\leq z\leq z_{max} \\ w=w_0,\ \ \text{at initial time.} \end{array}\right\} \tag{16}$$

The flow rate for both parent artery (Q_p) and daughter artery (Q_d) are obtained by the formulae

$$Q_p = 2\pi\ R\left[R\int_0^1 \xi\ w\ d\xi + R_2\int_0^1 w\ d\xi\right] \tag{17}$$

and

$$Q_d = \pi\ R\left[R\ \int_0^1 \xi\ w\ d\xi + R_2\ \int_0^1 w\ d\xi\right] \tag{18}$$

The impedance to unidirectional blood flow (resistive impedance) in the parent artery (λ_p) and daughter artery (λ_d) are calculated with

$$(\lambda_p)_i\ = \left|\frac{z_3\frac{dp}{dz}}{Q_p}\right|\ for\ z < z_3, \quad (\lambda_d)_i\ = \left|\frac{(z_{max} - z_3)\frac{dp}{dz}}{Q_d}\right|\ for\ z \geq z_3 \tag{19}$$

The shear stress along the walls of the artery is determined by using

$$\tau = \frac{\mu_f}{(1-\phi)^{2.5}}\ \frac{1}{R}\ \frac{\partial w}{\partial \xi}. \tag{20}$$

3. NUMERICAL SOLUTION

The Reduced equations (14) and (15) subjected to the boundary conditions (16) are solved numerically using finite-difference scheme. A three dimensional computational grid is imposed in $z - \xi - t$ plane. The stepping process is defined by $z_i = i\Delta z, i = 0, 1, \cdots, N$, $\xi_j = j\Delta\xi, j = 0, 1, \cdots, J$ and $t_k = k\Delta t, k = 0, 1, \cdots, M$ where Δz, Δt and $\Delta\xi$ are step lengths along the axial, time and radial directions respectively. If $w_{i,j,k}$ and $\Theta_{i,j,k}$ speak for the value of variables w and Θ at (z_i, ξ_j, t_k) respectively, then the derivatives are replaced with equivalent central difference approximations as given below.

$$\left.\begin{aligned}
&\frac{\partial w}{\partial \xi} = \frac{1}{2}[\frac{w_{i,j+1}^{k+1} - w_{i,j-1}^{k+1}}{2\triangle\xi} + \frac{w_{i,j+1}^{k} - w_{i,j-1}^{k}}{2\triangle\xi}],\\
&\frac{\partial^2 w}{\partial \xi^2}] = \frac{1}{2}[\frac{w_{i,j+1}^{k+1} - 2w_{i,j}^{k+1} + w_{i,j-1}^{k+1}}{(\triangle\xi)^2} + \frac{w_{i,j+1}^{k} - 2w_{i,j}^{k} + w_{i,j-1}^{k}}{(\triangle\xi)^2}],\\
&\frac{\partial w}{\partial t} = \frac{w_{i,j}^{k+1} - w_{i,j}^{k}}{\triangle t},
\end{aligned}\right\} \tag{21}$$

Similarly, we can write second order finite difference approximations for $\frac{\partial^2\Theta}{\partial\xi^2}$, $\frac{\partial\Theta}{\partial\xi}$ and $\frac{\partial\Theta}{\partial t}$.

Substituting (21) in (14) and (15), reduced to

$$(a_1)_{i,j}^k w_{i,j-1}^{k+1} + (a_2)_{i,j}^k w_{i,j}^{k+1} - (a_3)_{i,j}^k w_{i,j+1}^{k+1} + G_r\ \Theta_{i,j}^{k+1}\ =\ (r_1)_{i,j}^k \tag{22}$$

$$(b_1)_{i,j}^k \Theta_{i,j-1}^{k+1} + (b_2)_{i,j}^k \Theta_{i,j}^{k+1} + (b_3)_{i,j}^k \Theta_{i,j+1}^{k+1} =\ (r_2)_{i,j}^k \tag{23}$$

where

$$\left.\begin{aligned}
(a_1)^k_{i,j} &= -\tfrac{1}{4\,R\,\triangle\xi}\left[R_w^2\,p(k)+\tfrac{1}{(1-\phi)^{2.5}\,(\xi R+R_2)}\right]+\tfrac{1}{2\,R^2\,(\triangle\xi)^2\,(1-\phi)^{2.5}},\\
(a_2)^k_{i,j} &= -\left[H^2+\tfrac{R_w^2}{\triangle t}+\tfrac{1}{R^2\,(\triangle\xi)^2\,(1-\phi)^{2.5}}\right],\\
(a_3)^k_{i,j} &= \tfrac{1}{4\,R\,\triangle\xi}\left[R_w^2\,p(k)+\tfrac{1}{(1-\phi)^{2.5}\,(\xi R+R_2)}\right]+\tfrac{1}{2\,R^2\,(\triangle\xi)^2\,(1-\phi)^{2.5}},\\
(r_1)^k_{i,j} &= -(a_1)^k_{i,j}w^k_{i,j-1}+\left(\tfrac{1}{R^2(\triangle\xi)^2(1-\phi)^{2.5}}-\tfrac{R_w^2}{\triangle t}\right)w^k_{i,j}-(a_3)^k_{i,j}\,w^k_{i,j+1}+\tfrac{\partial p}{\partial z},
\end{aligned}\right\} \quad (24)$$

$$\left.\begin{aligned}
&(b_1)^k_{i,j} = -\tfrac{1}{4\,R\,\triangle\xi}\left[\tfrac{1}{\xi R+R_2}+p(k)\,R_w^2\,P_r^2\right]+\tfrac{1}{2\,R^2\,(\triangle\xi)^2},\\
&(b_2)^k_{i,j} = -\left[\tfrac{R_w^2\,P_r^2}{\triangle t}+\tfrac{1}{R^2\,(\triangle\xi)^2}\right],\quad (b_3)^k_{i,j} = \tfrac{1}{4\,R\,\triangle\xi}\left[\tfrac{1}{\xi R+R_2}+p(k)\,R_w^2\,P_r^2\right]+\tfrac{1}{2\,R^2\,(\triangle\xi)^2},\\
&(r_2)^k_{i,j} = -(b_1)^k_{i,j}\,\Theta^k_{i,j-1}+\left[\tfrac{1}{R^2\,(\triangle\xi)^2}-\tfrac{p_r\,R_w^2}{\triangle t}\right]\Theta^k_{i,j}\\
&-(b_3)^k_{i,j}\,\Theta^k_{i,j+1}-s\,(1+3\phi).
\end{aligned}\right\} \quad (25)$$

The equations (22) and (23) along with the boundary conditions (16) are shortened into a block tridiagonal system of equations and is solved by block elimination method.

4. RESULTS AND DISCUSSIONS

The aim of current study is to investigate the flow characteristics of blood through stenosed bifurcated artery under the consideration that blood as copper suspended nanofluid. For the better understanding of the analysis, used the following data: a = 5 mm, $d^{'}$ = 10 mm, l_0 = 5 mm, $\beta = \frac{\pi}{10}$, r_1 =0.51a, ϵ =2, H=0.2, s=0.2, $\mu_f = 0.894$, $P_r = 0.7$, $R_w^2 = 1.2$, $t = 2\ sec$ and $G_r = 0.3$. In figures fig. 2 to fig. 23 , the notation "$-n$" stands for fluid with nanoparicle volume fraction, "$-v$" stands for fluid without nanoparicle volume fraction for all the variables.

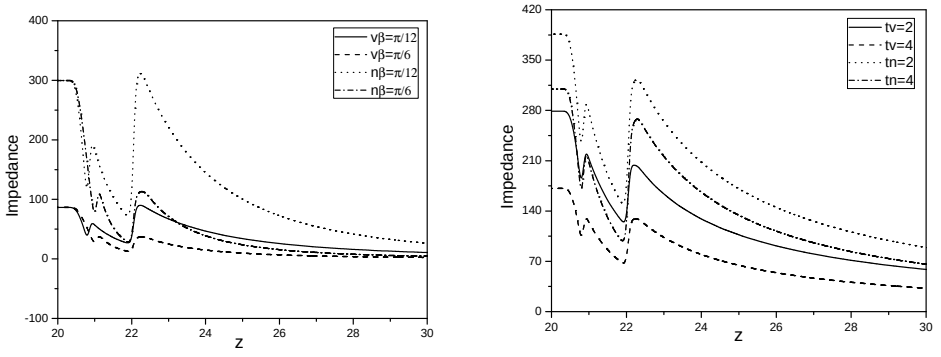

(a) **(b)**

Figure 2: Effect of (a) bifurcated angle β and (b) time t impedance with and without nanoparticle volume fraction on both sides of the apex for fixed values of s=0.2, $P_r = 0.7$, $R_w^2 = 1.2$, $G_r = 0.3$ and H=0.2.

The influence of half of the bifurcated angle β on impedance in daughter artery is presented in fig.2a. From this figure, it is observed that impedance is decreasing for higher values of β, but it is rising with an increase in the value of nanoparticle volume fraction. The variations of impedance with time near the apex is given in fig.2b. From this figure, it is noticed that impedance is diminishing for larger value of time (t), but it is increasing with the nanoparticle volume fraction.

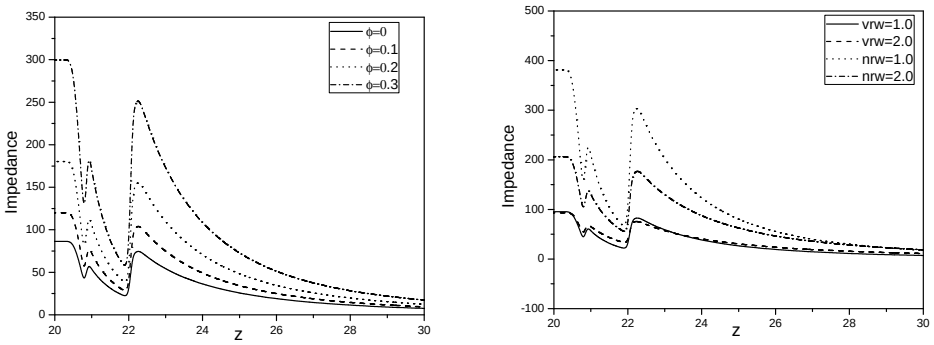

(a) **(b)**

Figure 3: Effect of (a) ϕ and (b) Womersley number on impedance with and without nanoparticle volume fraction on both sides of the apex for fixed values of s=0.2, $P_r = 0.7$, $\beta = \frac{\pi}{10}$, H=0.2, $G_r = 0.3$, and time t = 2 sec.

Figure 3a explores the influence of nanoparticle volume fraction on impedance near the flow divider. From this figure, it is clear that impedance is increasing with an advancement in the value of nanoparticle volume fraction. Fig. 3b disclose the influence of Womersley number R_w^2 on impedance with and without nanoparticle volume fraction near the flow divider. From fig. 2 to 3, it is noted that the impedance is decreasing with an advancement in the value of z, until inset of lateral junction, then a slight increase occurred suddenly, after that a gradual decrease till the apex, and again a sudden increase is observed. This is because of the divergence of blood flow at the bifurcation of artery. Thereafter, it is identified that the impedance is uniform till z_{max}.

The effect of (β) and H on flow rate both in parent and daughter arteries with and without nanoparticle volume fraction near the apex have been presented respectively in fig. 4a and 4b. From fig. 4a, it is seen that flow rate is higher for an increased value of β near the apex. Figure 4b reveals that the variations of flow rate with H is insignificant near the apex.

The variations of flow rate with nanoparticle volume fraction on both sides of the apex is plotted in fig.5a. From this figure, it is noticed that the flow rate is low for an increased value of ϕ on both sides of the apex. Reason being is that the density of

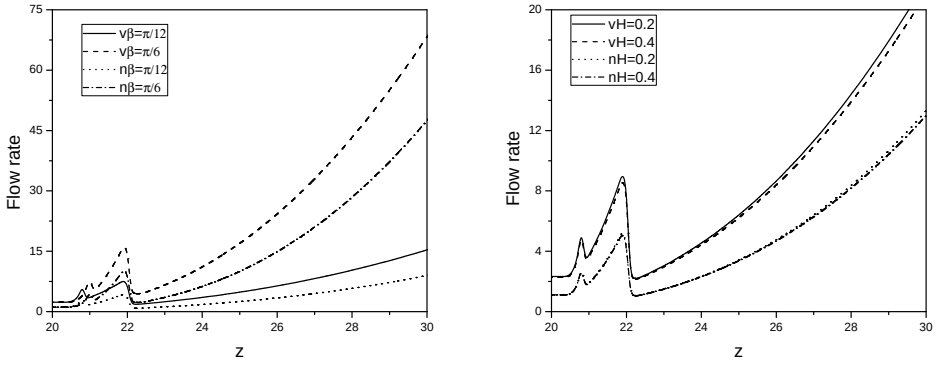

(a) **(b)**

Figure 4: Influence of (a) β and (b) magnetic parameter H on flow rate with and without nanoparticle volume fraction on both sides of the apex for fixed values of s=0.2, $P_r = 0.7$, $R_w^2 = 1.2$, $G_r = 0.3$ and time t = 2 sec.

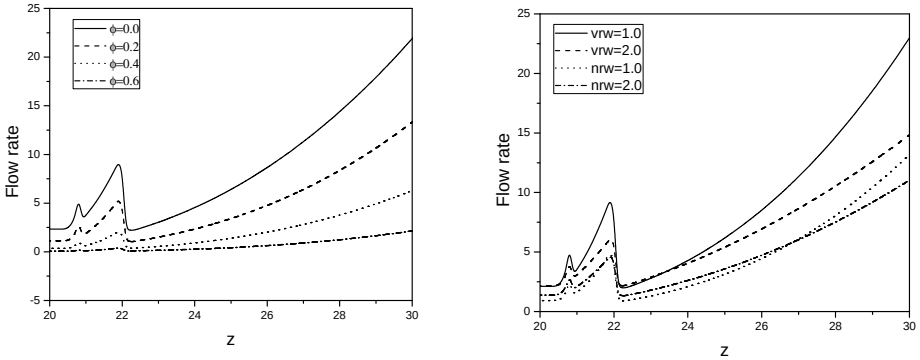

(a) **(b)**

Figure 5: Influence of (a) ϕ and (b) Womersley number on flow rate with and without nanoparticle volume fraction on both sides of the apex for fixed values of s=0.2, $P_r = 0.7$, $\beta = \frac{\pi}{10}$, H=0.2, $G_r = 0.3$, and time t = 2 sec.

copper suspended blood is higher than that of pure blood and it slows down the blood flow which is in turn decrease flow rate. This is useful in controlling the blood flow during the surgeries. Variations of flow rate with Womersley number on both sides of the apex with and without nanoparticle volume fraction is depicted in fig. 5b. This reveals that the flow rate is decreasing with an increase in the values of R_w^2 on both sides of the apex.

Figures 6a and 6b illustrate the influence of heat source parameter s and time t on flow rate with and without nanoparticle volume fraction near the flow divider. From these

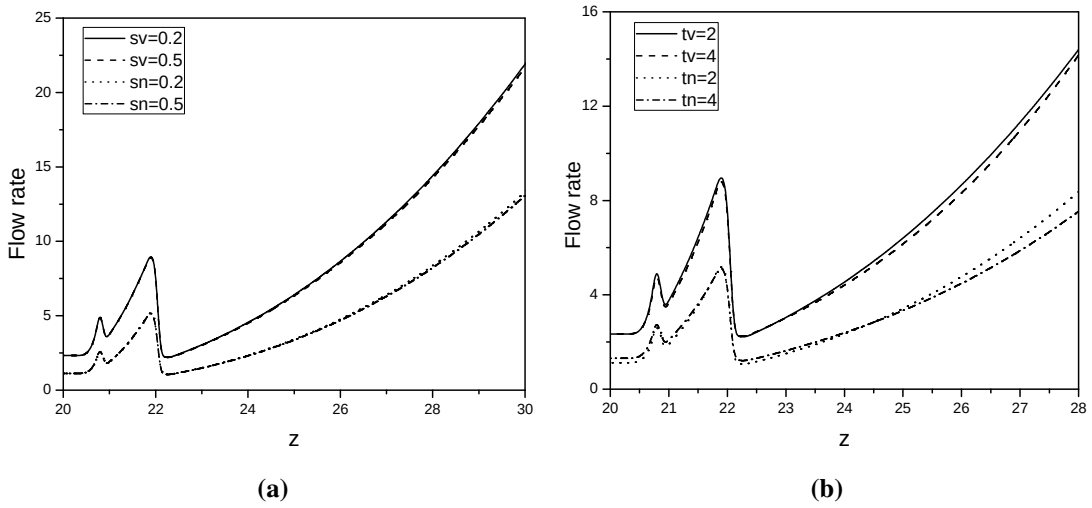

Figure 6: Effect of (a) heat source parameter s and (b) time t on flow rate with and without nanoparticle volume fraction on both sides of the apex for fixed values of $\beta = \frac{\pi}{10}$, H=0.2, $P_r = 0.7$, $R_w^2 = 1.2$ and $G_r = 0.3$.

figures, it is observed that the flow rate is decreasing with an increase in the values s and t on both sides of the apex. But effect of s and t are trivial on flow rate. From fig 4 to 6, it is noticed that the flow rate profiles are locally increasing till inset of the lateral junction, then a small decrease is identified and again increase until the apex. Thereafter, these patterns found to be steady till z_{max}. It is noticed that flow rate is increasing in case of pure blood as compared to copper suspended blood, because the density of Copper suspended blood is more than that of pure blood and it slows down blood flow and decrease flow rate.

The effect of β on shear stress along inner and outer walls of the daughter artery with and without nanoparticle volume fraction is presented in fig. 7a and 7b. From these figures, it is identified that shear stress increases with an increase in the value of β along the inner and outer walls of the daughter artery.

The effect of H on shear stress along both walls of daughter artery with and without nanoparticle volume fraction is depicted in figs. 8a and 8b. From these figures, it is noticed that the effect of H on shear stress is almost negligible along the inner and outer walls of the daughter artery.

Figures 9a and 9b explore the effect of ϕ on shear stress along the inner and outer wall of the daughter artery without nanoparticle volume fraction. From these figures, it is seen that the shear stress is decrease along the inner wall and increase along the outer

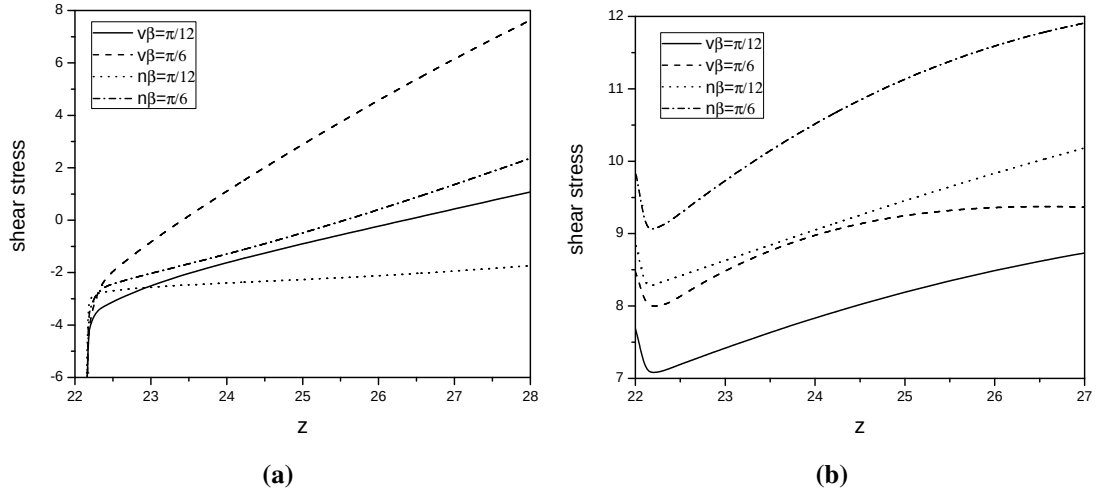

Figure 7: Influence of β on shear stress (a) along the inner and (b) outer walls of daughter arterytime for fixed values of other parameters

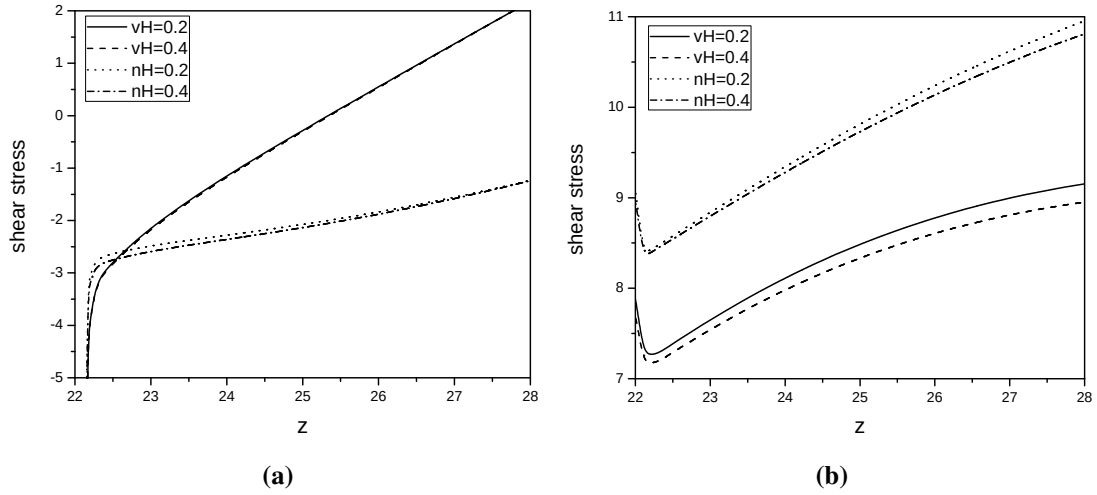

Figure 8: Influence of H on shear stress (a) along the inner and (b) outer walls of daughter arterytime for fixed values of other parameters

wall of daughter artery with an increase in the value of ϕ.

The variations of shear stress with Womersley number along the walls of daughter artery with and without nanoparticle volume fraction are described in figs. 10a and 10b. From these figures, it is worth to mention that shear stress is rising along the inner wall and falling along the outer wall of the daughter artery with an increase in the value of Womersley number.

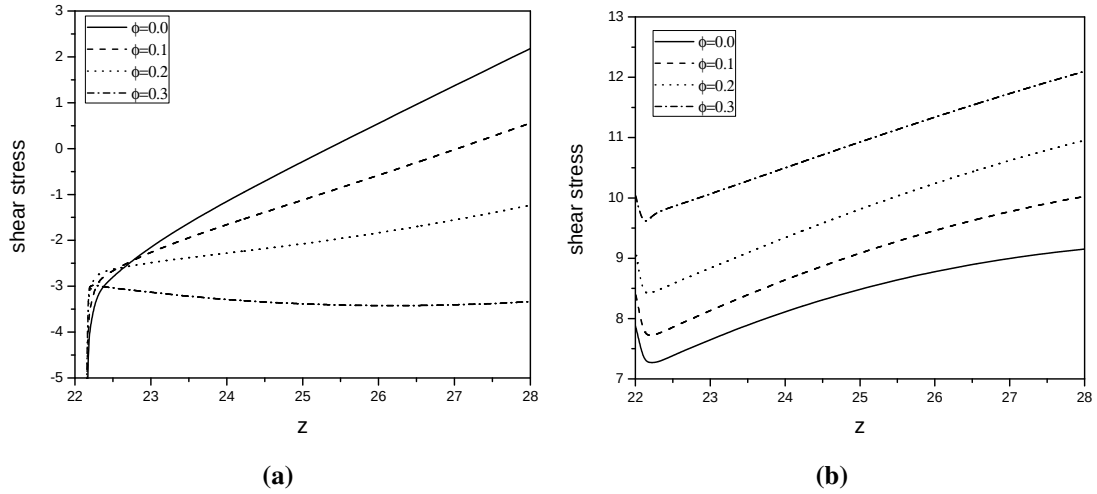

Figure 9: Influence of ϕ on shear stress (a) along the inner and (b) outer walls of daughter arterytime for fixed values of other parameters

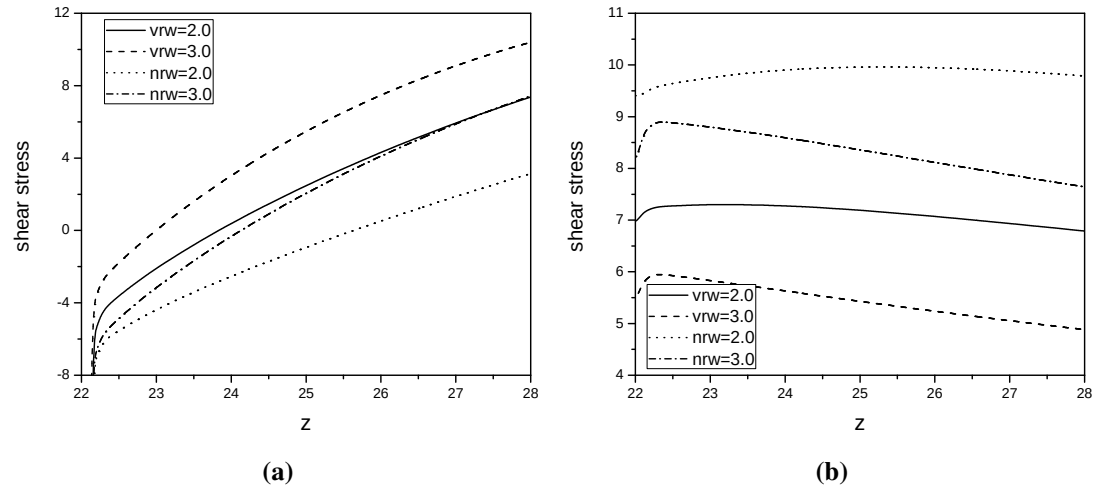

Figure 10: Influence of rw on shear stress (a) along the inner and (b) outer walls of daughter arterytime for fixed values of other parameters

Figures 11a and 11b explore the effect of heat source parameter on shear stress along the boundary of daughter artery. The effect of s is almost similar to that of H on shear stress along the inner and outer wall of the daughter artery. It is observed from figs. 7 to 11 that shear stress is decreasing along the inner wall and increasing along the outer wall for increased value of nanoparticle volume fraction.

Figures 12a and 12b explore the effect of impedance with and without nanoparticle

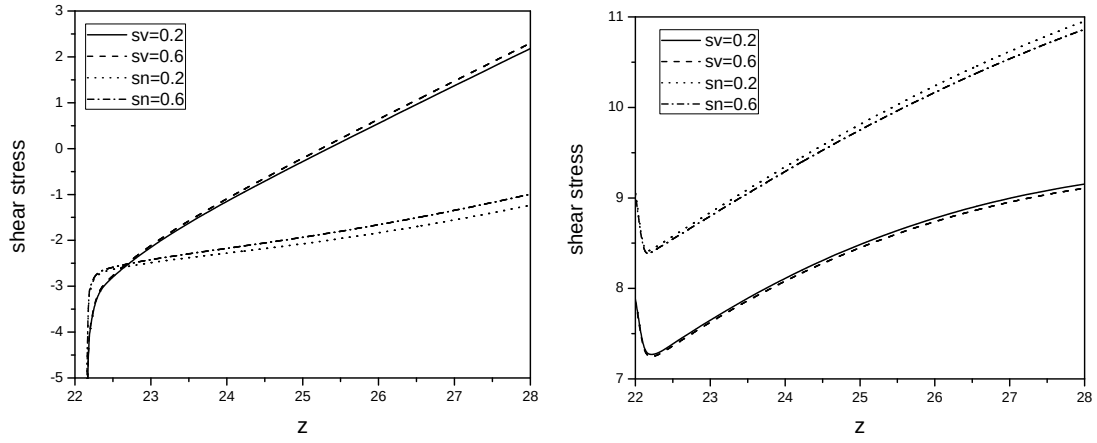

Figure 11: Influence of s on shear stress (a) along the inner and (b) outer walls of daughter arterytime for fixed values of other parameters

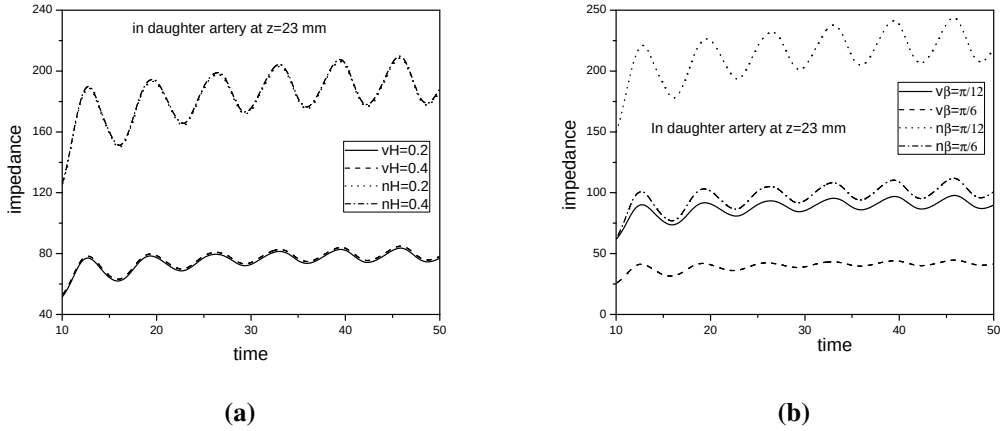

Figure 12: Variations of impedance against time (pulsatile nature) with (a) H and (b) β with and without nanoparticles volume fraction for fixed values of other parametes

volume fraction against pulsatile nature with Hartmann number and half of the bifurcated angle in the daughter artery. From fig. 12a, it is observed that the impedance is enhancing with nanoparticle volume fraction and magnetic parameter in daughter artery, but effect of H is very trivial. Figure 12b explains that impedance is decreasing with an increase in the value of β and also in the value of ϕ in daughter artery near to the apex.

The variations of flow rate with and without nanoparticle volume fraction against

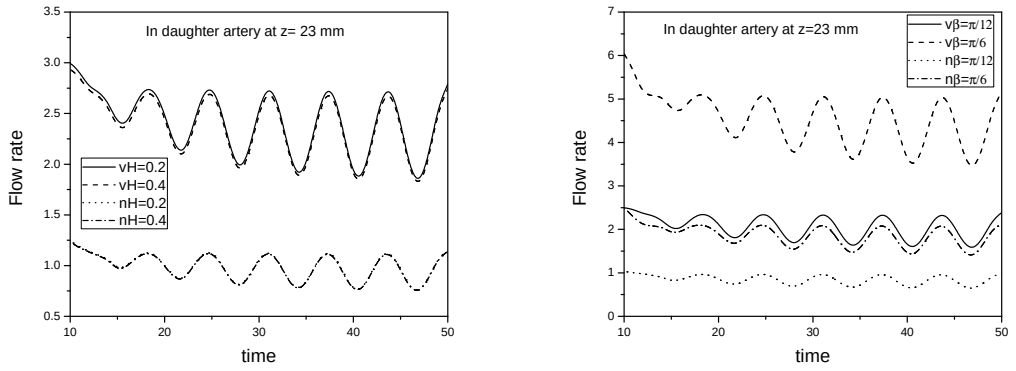

(a) **(b)**

Figure 13: Variations of flow rate against time (pulsatile nature) with (a) H and (b) β with and without nanoparticles volume fraction for fixed values of other parametes

pulsatile nature with H and β are depicted in fig. 13a and 13b respectively. From fig. 13a, it is noticed that flow rate is diminishing with an increase in the value of ϕ and H, but the effect of H is almost negligible. From fig. 13b, it is clear that flow rate is increasing with an increase in the value of β, but decrease in the value of ϕ in daughter artery.

5. CONCLUSIONS

The present study reveals and concludes the influence of β, ϕ and s on physical quantities such as flow rate, impedence and shear stress.

- Impedance has been increasing with an increase in the value of ϕ, R_w and decrease in the value of β, time (t) on both sides of the apex.
- Flow rate has been increasing with an increase in the value of β and decrease in the value of ϕ, R_w, H, t on both sides of the apex.
- Shear stress has been increasing with an increase in the values of β, R_w and s and decrease with an advancement in the value of H, ϕ along the inner wall of the daughter artery. But along the outer wall of the daughter artery shear stress increases with an increase in the value of β, ϕ and it's decrease with an increase in the value of H, R_w, s.

REFERENCES

[1] Choi. S.U.S. and Eastman. J.A., "Enhancing thermal conductivity of fluids with nanoparticles", *The Proceedings of the ASME International Mechanical*

Engineering Congress and Exposition, ASME, San Francisco, USA, FED 231/MD 66, 99–105, 1995.

[2] Kalidas Das., "Slip flow and convective heat transfer of nanofluids over a permeable stretching surface", *Computers & Fluids*, vol 64, 2012, pp. 34-42.

[3] Ellahia. E., Rahmanb. S.U., Nadeemc. S., "Blood flow of Jeffrey fluid in a catherized tapered artery with the suspension of nanoparticles", *PhysicsLettersA*, vol 378, 2014, pp. 2973—2980.

[4] Akbar. N. S., Rahman S. U., Ellahi. R. and Nadeem. S., "Nano fluid flow in tapering stenosed arteries with permeable walls", *"International Journal of Thermal Sciences"*, Vol. 85, 2014, pp. 54-61.

[5] Nadeema. S. and Ijaz. S., "Nanoparticles analysis on the blood flow through a tapered catheterized elastic artery with overlapping stenosis", *Eur. Phys. J. Plus*, Vol. , 2014, pp. DOI 10.1140/epjp/i2014-14249-1.

[6] Akbar. N. S., and Mustafa. M. T., "Ferromagnetic effects for nanofluid venture through composite permeable stenosed arteries with different nanosize particles", *AIP Advances*, Vol. 5, 2015, Paper ID. 077102 (9 pages).

[7] Srinivasacharya. D. and Madhava Rao. G., "Magnetic Field Effects for Copper Suspended Nanofluid Venture Through a Bifurcated Artery", *"Journal of Nanofluids"*, vol.5, 2016, pp.774–782.

[8] Kolin. A., "An electromagnetic flow meter: Principle of the method and its application to blood flow measurements",*"Experimental Biology and Medicine"*, Vol. 35, 1936, pp. 53–56.

[9] Korchevskii. E. M. and Marochnik. L. S., "Magnetohydrodynamic version of movement of blood",*Biophysics,*, Vol. 10, 1965, pp. 411—413.

[10] Hatami. M., Hatami. J. and Ganji. D. D., "Computer simulation of MHD blood conveying goldnanoparticles as a third grade non-Newtoniannanofluid in a hollow porous vessel", *"Computer Methods and Programs in Biomedicine"*, Vol. 113, 2014, pp. 632—641.

[11] Jayati. T., Vasua. B., Anwar. B., Rama Subba Reddy. G and Kameswaran., P.K., "Computational simulation of rheological blood flow containing hybrid nanoparticles in an inclined catheterized artery with stenotic, aneurysmal and slip effects",*"Computers in Biology and Medicine"*, Vol. 139, 2021, 105009, doi.org/10.1016/j.compbiomed.2021.105009

[12] Hussain. A,, Sarwar. S., Rehman. A., Akbar. S., Gamaoun. F., Coban. H., Abdulrazak H., and Alqurashi. M.S., "Heat Transfer Analysis and Effects of (Silver and Gold) Nanoparticles on Blood Flow Inside Arterial Stenosis", *Applied Sciences*, Vol. 12(3), 2022, 1601; https://doi.org/10.3390/app12031601.

[13] Garg. J., Poudel. B., Chiesa. M., Gordon. J. B., Ma. J. J., Wang. J. B., Ren. Z. F., Kang. Y. T., Ohtani. H., Nanda. J., McKinley G. H. and Chen.G, "Enhanced thermal conductivity and viscosity of copper nanoparticles in ethylene glycol nanofluid", *Journal of Applied Physics* , vol 103, 2008, pp. 074301–074306.

[14] Chakravarty. S. and Mandal P. K., "An Analysis of Pulsatile Flow in a Model Aortic Bifurcation", *Int. J. Engg. Sci.*, Vol. 35(4), 1997, pp. 409-422.

[15] Chakravarty. S., and Sen. S., "A mathematical model of blood flow in a catheterized artery with a stenosis", *Journal of Mechanics in Medicine and Biology*, vpl. 9 (3), 2012, pp.377-410.

[16] Srinivasacharya. D. and Madhava Rao. G., "Mathematical model for blood flow through a bifurcated artery using couple stress fluid", *"Mathematical Biosciences*, vol.278, 2016, pp.37–47".

[17] Shit. G.C., and Roy. M., "Pulsatile flow and heat transfer of a magneto-micropolar fluid through a stenosed artery under the influence of body acceleration", *J of Mech in Medicine and Biology*, Vol. 11, 2011, pp.643–661.